

Ultrafast midinfrared laser system for enhanced self-amplified spontaneous emission applications

R. Tikhoplav* and A. Murokh

RadiaBeam Technologies, Santa Monica, California 90404, USA

A. Lentner

School of Nuclear Engineering, Purdue University, West Lafayette, Indiana 47907, USA

I. Jovanovic

Department of Mechanical and Nuclear Engineering, The Pennsylvania State University, University Park, Pennsylvania 16802, USA

(Received 9 August 2010; published 29 July 2011)

Of particular interest to x-ray free-electron laser light source facilities is the enhanced self-amplified spontaneous emission (ESASE) technique. ESASE requires an ultrafast (20–50 fs), high peak power, high repetition rate, reliable laser system working in the midinfrared spectral range ($\geq 2 \mu\text{m}$). These requirements can be met by a novel ultrafast midinfrared laser system based on optical parametric chirped-pulse amplification (OPCPA). OPCPA is a technique ideally suited for production of ultrashort laser pulses at the center wavelength of $2 \mu\text{m}$. Some of the key features of OPCPA are the wavelength agility, broad spectral bandwidth, and negligible thermal load. The ESASE-compatible laser technology analysis and the preliminary OPCPA simulation results are presented.

DOI: 10.1103/PhysRevSTAB.14.070704

PACS numbers: 41.60.Cr, 41.75.-i, 42.65.Yj, 42.55.Vc

I. INTRODUCTION

For the past decade, free-electron laser (FEL)-based light sources have become an increasingly indispensable tool in innovative ultrafast x-ray research that has proven to be beneficial in areas ranging from atomic and molecular sciences to chemical, materials, and biological studies. Such light sources are employed or being built in a number of laboratories worldwide: SLAC Linac Coherent Light Source (LCLS) [1,2], European XFEL [3,4], and SPring-8 [5], to name a few. The enhanced self-amplified spontaneous emission (ESASE) technique has great potential to benefit the FEL-based light sources. ESASE has the following principle of operation: an optical laser interacts with the electron beam in an upstream wiggler and induces energy modulation, which is converted to a large density modulation prior to entering the SASE undulator [6]. Such modulated electron beam has high current pockets which exhibit a significantly shorter SASE gain length, allowing for saturation with subfemtosecond slippage and, hence, the generation of ESASE attosecond x-ray spikes. The use of the optical laser also provides natural synchronization for pump-probe experiments. Because of these features, implementation of the proposed ESASE scheme at the existing and future fourth generation light source

facilities can become an essential tool for probing transient processes in condensed matter on an atomic scale [7].

In this paper a novel approach is described to develop an optical modulation laser suitable for ESASE application at LCLS. The main technological challenge for such laser is achieving ultrafast pulses at long wavelengths of $\sim 2 \mu\text{m}$ or more. An unconventional wavelength requirement is a consequence of optimization of the ESASE FEL process, discussed in detail in Ref. [6] specifically in the context of the LCLS system parameters. While discussion of the FEL dynamics in the ESASE regime is outside the scope of this manuscript, below we summarize the argument in Ref. [6], which discusses the nature of limitations on the ESASE optical wavelength.

To obtain ESASE at LCLS, a 2 GeV energy was chosen for the optical modulation process, so that the beam is soft enough to induce large energy spread with the moderate laser power in a relatively short wiggler (Fig. 1). A modulated beam is then accelerated to the operating energy of $\sim 15 \text{ GeV}$, where it undergoes longitudinal compression in a magnetic chicane, and is finally injected into the x-ray SASE undulator. In order for the ESASE scheme to work efficiently, the duration of the ESASE enhanced current

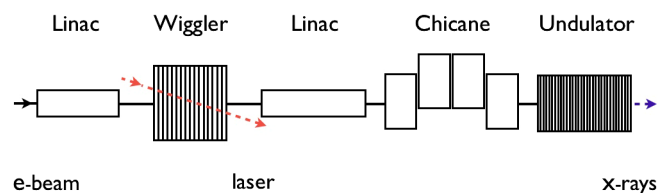


FIG. 1. ESASE schematics; adapted from [6].

*rodion@radiabeam.com

Published by the American Physical Society under the terms of the *Creative Commons Attribution 3.0 License*. Further distribution of this work must maintain attribution to the author(s) and the published article's title, journal citation, and DOI.

beamlets has to be longer than the amount of SASE slippage through saturation. For a typical short-wavelength FEL, the saturation occurs at about eight FEL field gain lengths, with the corresponding slippage value estimated in [6] at about 80–100 nm. At the same time, the beamlet compression efficiency of the optimized wiggler-chicane system is only limited by uncorrelated energy spread (in the single digit keV range for LCLS) and for a reasonably large linear energy modulation in the wiggler, the compression ratio in the chicane can be as large as a factor of 20. Hence, in order to achieve the optimized efficiency of the ESASE process, the laser wavelength should comfortably exceed the product of the maximum slippage length and the compression ratio. More specifically to the LCLS parameters, a SASE slippage of $100 \text{ nm} \times 20$ yields optical laser wavelength to be no less than $2 \mu\text{m}$ (but also not too much longer to preserve Fourier-transform-limited temporal coherency in x-ray lasing pulses). Such wavelength limitation combined with ultrashort pulse requirements presents a significant engineering challenge, the solution to which is proposed herein.

So far, the discussion was limited to a linear dynamics in the ESASE system, with the efficiency of the modulation and compression mechanisms limited by the intrinsic energy spread and emittance of the electron beam. While the focus of this work is on the robust, commercial components based, mid-IR laser system development for ESASE, a brief review of some additional important limitations of the ESASE approach is necessary, as it may affect the system design decisions in the future. First of all, we assume that the collective effects, such as coherent synchrotron radiation, in the chicane, as well as higher order effects in the transport would not degrade the beam brightness within the working section (WS), as defined in [6], by the time the beam reaches the undulator. Such an assumption is generally consistent with the dynamics of the LCLS-type beam, which is very stable due to a very large Lorentz factor. For a practical development of the ESASE scheme, rigorous numerical simulations and error analysis in the exact beam line configuration will be necessary to remove this risk, although this part of the system design is outside the scope of this manuscript.

In addition, the high current spike generated in the middle of the WS will be subject to the longitudinal space charge forces, which may impose an additional limit on the maximum compression efficiency in the ESASE scheme. This problem is somewhat similar to the problem of debunching of the electron beam following the prebuncher for the inverse free-electron laser, for which detailed treatment is given in [8]. In that case, to the first order, longitudinal space charge is frozen, when the distance between the prebuncher (a compression chicane in our case) and the undulator entrance should be not larger than a fraction of the e-beam plasma wavelength. For the LCLS-type beam of 15 GeV, with the transverse rms size on the order of

$\sigma_x \approx 30 \mu\text{m}$, and the peak current $I_p \approx 3.4 \text{ A}$, the plasma wavelength, λ_p , outside the WS region yields a relatively large value $\lambda_p \approx \pi \sigma_x \sqrt{I_A \gamma^3 / I_p} \approx 1.1 \text{ km}$, and the corresponding debunching length of few hundred meters. On the other hand, inside the high current spike within the WS, the debunching length could be reduced by as much as a factor of 4, and become comparable to the ESASE saturation length in the undulator. As a result, for the scheme to work efficiently with the stated beam parameters, the distance between the chicane exit and the undulator entrance should be reduced to 10–20 meters.

II. OPCPA LASER TECHNOLOGY

Optical parametric chirped-pulse amplification (OPCPA) is a technique ideally suited for production of ultrashort laser pulses at the center wavelength of $2 \mu\text{m}$. In OPCPA, an efficient energy transfer between the short-wavelength pump pulse and the long-wavelength signal pulse is realized through a three-wave mixing process in a nonlinear medium (a solid-state crystal such as beta-barium borate, lithium triborate, or potassium dihydrogen phosphate are typically used). Some of the key features of OPCPA are the wavelength agility, broad spectral bandwidth, and negligible thermal load. The main challenge associated with the use of OPCPA has always been the availability of suitable pump lasers producing relatively short pulses and the pump-signal synchronization. Since OPCPA is an instantaneous process with no energy storage, the pump pulse duration needs to be comparable to the pulse duration of the signal pulses; synchronization must be realized to within a small fraction of the signal pulse. This is very challenging for shorter pump pulses needed in chirped-pulse amplification, especially if the seed and pump pulses originate from different lasers.

Unlike the schemes proposed to date [9] and capable of generating ultrashort $2 \mu\text{m}$ pulses, there is no need for design and construction of a new pump laser system but rather the same, commercially available 800 nm Ti:sapphire laser will be used to produce pump pulses and to pump a nondegenerate OPCPA operated with relatively small chirp, within approximately $100\times$ of the transform-limited pulse duration. Such an approach is beneficial from both simplicity and cost-efficiency points of view.

The schematic of the proposed approach is shown in Fig. 2. Here, a pulse generated by a Ti:sapphire laser system is split into two pulses of unequal energies. The high-energy pulse is used to pump the OPCPA and the low-energy pulse is injected into a photonic crystal fiber or a simple bulk nonlinear medium, where it is spectrally broadened by self-phase modulation (SPM). The pulse with broadened spectral content is then passed through an appropriate spectral filter to select the wavelengths in the vicinity of $1.33 \mu\text{m}$ for use as seed pulses for OPCPA.

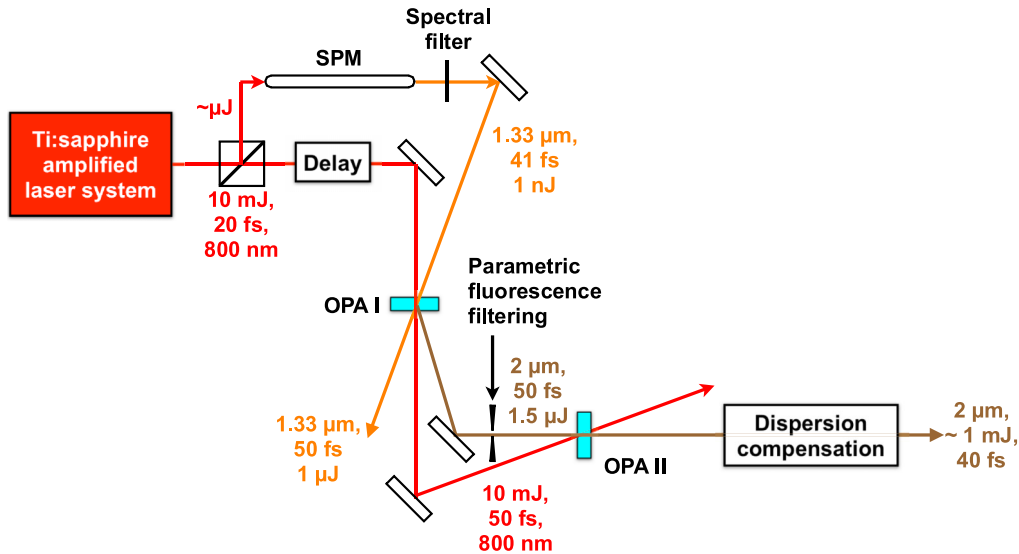


FIG. 2. Nondegenerate $2\ \mu\text{m}$ OPCPA system pumped by a standard Ti:sapphire ultrafast laser system that consists of two stages. The first stage is seeded with a Gaussian beam in both space and time; the spectrum is also assumed to be Gaussian with no incident chirp. Since the first stage is unsaturated the output beam is Gaussian in both space and time as well. The second OPA is saturated and will be seeded with a pulse having a transverse shape of a super-Gaussian as well as a chirp that will be compensated after amplification using a dispersion compensation scheme.

This seeding method is the first important innovation in our approach: instead of using SPM to spectrally shift and broaden the $800\ \text{nm}$ pulse to $2\ \mu\text{m}$, SPM is used to produce a spectral shift only to $1.33\ \mu\text{m}$. The $1.33\ \mu\text{m}$ pulse is used in the first stage of OPCPA to produce the required $2\ \mu\text{m}$ pulse in the idler beam *concurrently with amplification*. The difference-frequency process used is $800\ \text{nm} \rightarrow 1333\ \text{nm} + 2000\ \text{nm}$, and the $2000\ \text{nm}$ pulse is generated as the idler beam in the first stage of OPCPA. This more modest spectral shift significantly relaxes the requirements on the peak power and pulse energy in the spectral broadening medium, thus reducing the probability of optical damage, increasing the stability, and reducing the complexity of subsequent dispersion compensation needed for recompression of amplified pulses near Fourier-transform limit. In the subsequent OPCPA stage(s), the $2\ \mu\text{m}$ pulse will be used in a standard configuration (as a signal beam), which does not require compensation of angular dispersion at the output of the second amplifier stage. The scheme of idler-seeding has been previously successfully demonstrated [10] in a nearly degenerate OPCPA and is thus expected to be applicable to this approach even when the optical parametric amplifier is operated further from its degeneracy point.

To ensure optimized matching, a resizing telescope will be implemented before each OPCPA stage. Also, a delay line consisting of translatable mirrors will be used to optimize the seed-pump overlapping.

The three-wave mixing process is highly nondegenerate, which normally results in an undesirable narrow gain bandwidth in conventional collinear beam configurations. Here we introduce another innovation that will allow

production of $2\ \mu\text{m}$ pulses with broad spectral bandwidth from OPCPA in this scheme. Similar to prior work [9], it is proposed to use a noncollinear three-wave mixing configuration, but in conjunction with the use of the idler wave instead of the signal wave at the output of the first amplifier stage. As a result, the generated idler beam at the output of the first amplifier stage will have angular dispersion (Fig. 3), which will be compensated before injection into the next OPCPA stage by the use of a prism or grating.

Choosing the crystal type and the noncollinear angle is critical for optimization of the amplified signal bandwidth and pulse energy. A number of promising candidates for nonlinear crystals exist. Preliminarily, our design focuses on the crystal beta-barium borate (BBO), which shows a potential in this application with its relatively short interaction length needed to produce the required pulse energies

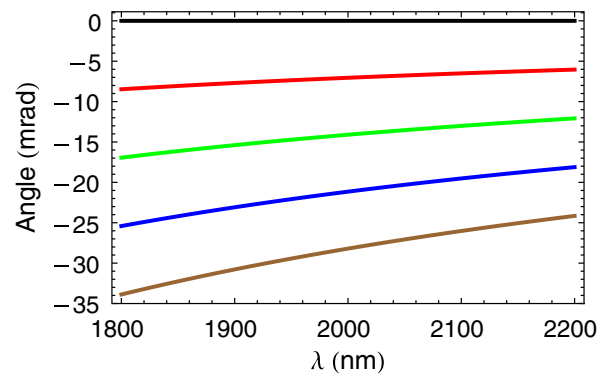


FIG. 3. Angular dispersion of the idler beam in the first BBO OPCPA stage, for various noncollinear angles: 0° -black, 2° -red, 3° -green, 4° -blue, 5° -brown.

and the relatively broad calculated bandwidth in the preliminary work. For such short interaction lengths, the transparency of the BBO crystal at $\sim 2 \mu\text{m}$ is expected to be adequate. For example, the BBO crystal absorption coefficient at $2.09 \mu\text{m}$ is 0.07 cm^{-1} and $<0.01 \text{ cm}^{-1}$ for o-rays and e-rays, respectively [11].

The second innovation is the use of chirped-pulse pumping. Unlike many OPCPA configurations that utilize relatively narrow-bandwidth pump sources, our approach exhibits an additional degree of freedom arising from the possible use of pump pulse chirp to produce *temporally variable phase matching*. By the use of both pump and signal chirp, it is possible to partially compensate for the phase mismatch, as different pump wavelengths can be overlapped with different signal wavelengths, as previously demonstrated for use in seeding high-energy OPCPA [12,13]. We illustrate this point in Fig. 4, where we plot the function $\text{sinc}^2(\Delta kL/2)$ against the deviation of pump and signal wavelength from their center wavelengths of $0.8 \mu\text{m}$ and $2 \mu\text{m}$, respectively. To the first order, this function is proportional to the conversion efficiency in the nonlinear mixing process, where Δk is the wave vector mismatch among the signal, idler, and pump, and L is the length of medium. For this example, we choose a typical length such as $L = 1 \text{ mm}$. Apparently, for short pulse durations such as the ones needed for ESASE, and using the collinear nondegenerate frequency mixing process shown here, it would be possible to obtain broader spectral bandwidth and shorter pulse durations if the center wavelengths of signal and pump can be appropriately matched to each other.

Opportunity to perform such matching exists, since the seed pulse produced by SPM will be accompanied by chirp, and without dispersion compensation will be longer than the pump pulse used to produce the seed pulse by SPM. Thus, a chirp will be needed on the pump pulse split from the same Ti:sapphire laser to match the pulse duration

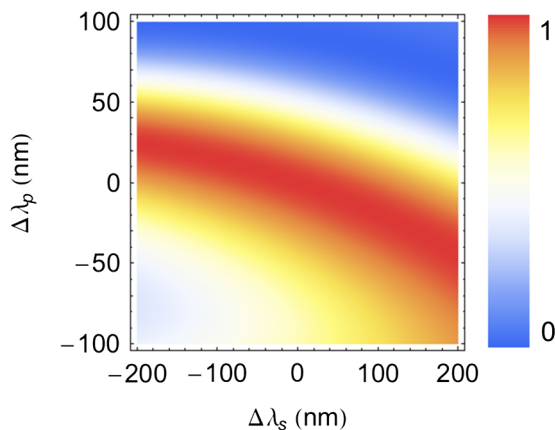


FIG. 4. Phase mismatch-induced efficiency factor $\text{sinc}^2(\Delta kL/2)$ as a function of signal and pump wavelength, when a 1 mm long BBO crystal is optimized for the type I mixing process $2000 \text{ nm} + 1333 \text{ nm} = 800 \text{ nm}$.

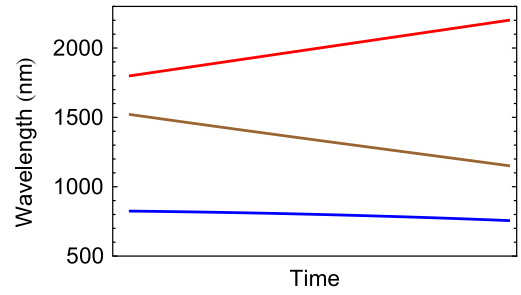


FIG. 5. Chirp can be used on both the signal and the pump to optimize the phase matching. For a linear chirp of the signal (red), the calculation shows the required chirp of the pump (blue) and the resulting idler (brown) needed to obtain perfect phase matching in a BBO crystal optimized for the type I mixing process $2000 \text{ nm} + 1333 \text{ nm} = 800 \text{ nm}$.

of the seed pulse. In addition, if this chirp is of appropriate magnitude and sign, much broader spectral bandwidths can be supported. In Fig. 5 we show the results of a simple calculation of the chirp of the pump needed to produce ideal phase matching when the chirp of the signal is nearly linear and positive, as expected from the very dispersive SPM process.

The mismatch between the pump and seed chirp will be imprinted on the idler pulse, offering an opportunity for convenient shaping of the idler phase for simple pulse compression at the output of the second amplifier. This spectral phase engineering requires good synchronization between the signal and the pump pulse, a requirement clearly satisfied in our approach, which utilizes the same pump laser as the source for both the signal and the pump pulse.

High-gain OPCPA is known to produce a significant parametric fluorescence background. In the case of our design, this fluorescence background will have the pulse duration nearly identical to that of the amplified signal, but can reduce the available pump energy available for signal amplification. This fluorescence will be suppressed by separating the amplification process into several amplification stages, with careful spatial filtering between stages. With a typical gain of $\sim 10^3$ – 10^4 per stage, two stages are normally needed to arrive with the desired pulse energy in the range of a mJ.

III. OPTICAL SIMULATIONS

Modeling of the broad-bandwidth difference-frequency process ($800 \text{ nm} \rightarrow 1333 \text{ nm} + 2000 \text{ nm}$) used to produce $2 \mu\text{m}$ pulses is of paramount importance for the implementation of the proposed laser system. We modeled a noncollinear OPCPA process using a ubiquitous BBO crystal pumped by 800 nm pulses, using a simplified numerical model. The results indicate that the bandwidth of the process is sufficiently high to support production of ultrashort laser pulses at $2 \mu\text{m}$, even without the use of

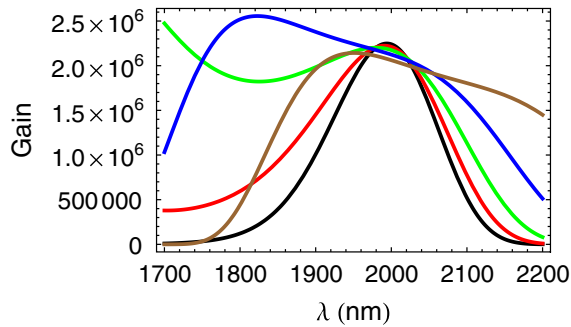


FIG. 6. Spectral bandwidth in 7.5 mm gain length of BBO OPCPA pumped by 800 nm pulses at 10 GW/cm^2 , at noncollinear angles of: 0° -black, 2° -red, 3° -green, 4° -blue, 5° -brown.

chirped-pulse pumping and large noncollinear angles. For a $\sim 4^\circ$ external noncollinear angle, the bandwidth of the process is optimized (Fig. 6). A code was specifically adapted for this task from the prior work by one of the authors [14,15]. The code is based on the numerical solution of coupled wave equations for difference-frequency mixing, with dispersion effects in birefringent or quasi-phase-matched nonlinear crystals taken into account. The code makes use of the nonlinear Snell's law to make predictions on the spectral bandwidth in complex noncollinear three-wave mixing configurations, and has been extensively tested in prior work [16–18], including the first demonstration of noncollinear OPCPA [19].

Complete analysis of the system requires dispersion modeling and design of appropriate dispersion compensation. In our system the dispersion will be dominated by the SPM in producing the $1.33 \mu\text{m}$ seed pulse. The details of dispersion management depend on the exact scheme chosen for spectral broadening and the associated type and length of the SPM medium. It is anticipated that the required dispersion compensation will be small in magnitude, and will be accomplished at the output of the SPM stage of the system. Subsequent OPCPA system stages exhibit short gain lengths and thus will not significantly contribute to pulse broadening. The effect of angular dispersion in OPCPA and pulse front tilt is the integral component of the comprehensive OPCPA code [14], which has been extensively tested in experiments. This code does not only allow for the accurate prediction of the pulse front tilt effects and angular dispersion, but is also a complete three-dimensional code that allows detailed calculation of OPCPA energetics with temporally and spatially nonuniform pump and signal beams that are used in real experiments. While this code also takes into account diffraction, this effect is not expected to be very pronounced due to the short interaction length in nonlinear crystals.

With good dispersion compensation producing nearly Fourier-transform-limited pulses, the anticipated pulse duration of the seed will not substantially increase in the broadband OPCPA process. The amplification is modeled using 10 GW/cm^2 800 nm pulses in 7.5 mm total gain

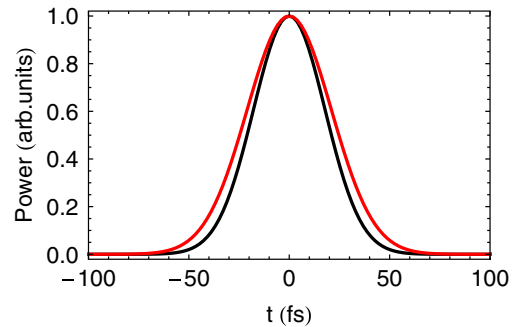


FIG. 7. Calculated Fourier-transform-limited normalized pulse shape before (black) and after (red) OPCPA. The total gain length in BBO is 7.5 mm, and the OPCPA is pumped by 10 GW/cm^2 800 nm pulses. Injection of a 41 fs seed pulse results in a 50 fs amplified pulse.

length of BBO OPCPA, assuming an input seed pulse from SPM and spectral filtering on the order of 1 nJ. The injected spectrum is assumed to be Gaussian, with the spectral width consistent with a 41 fs transform-limited pulse duration. No incident pulse chirp is assumed in this calculation. A gain of $\sim 10^6$ is needed to produce the required 50 fs pulse. As shown in Fig. 7, injection of a 41 fs pulse into OPCPA is calculated to produce a 50 fs pulse even at a noncollinear angle set to $\sim 0^\circ$.

To simulate the effects of beam profile, dispersion, and group velocity dispersion on the spatial and temporal beam profile of the amplified signal and to estimate the conversion efficiency, we have utilized the nonlinear code SNLO [20]. The first optical parametric amplification (OPA) stage is unsaturated and the input as well as the output are Gaussian in both space and time. In our simulations the second OPA is seeded with a pulse having a transverse shape of a fourth-order super-Gaussian, which can easily be obtained by using a soft aperture; the longitudinal shape of the seed for the second OPA is kept Gaussian. We have found that the use of the fourth-order super-Gaussian beam profile results in significantly better conversion efficiency compared to the Gaussian beam profile. For the following calculations we focus on the final optical parametric amplifier BBO crystal, in which we require a gain on the order of 10^3 to amplify the $\sim 1 \mu\text{J}$ signal obtained from the first optical parametric amplifier. The input pump energies of the signal and pump are $1 \mu\text{m}$ and 10 mJ, respectively, pulses have transform-limited 50 fs FWHM, Gaussian spectrum and no chirp, and the beams are fourth-order super-Gaussian spatially with $1/e^2$ full width of 10 mm. The injected signal is delayed with respect to the pump by 100 fs to partially compensate for the differences of group velocity dispersion among the three waves. The maximum theoretical conversion efficiency that can be realized in this difference-frequency mixing process is 40%. A more conservative estimate for conversion efficiency expected from this process involves the imperfect spatial and temporal overlap of pulses and nonuniform beam profiles and would

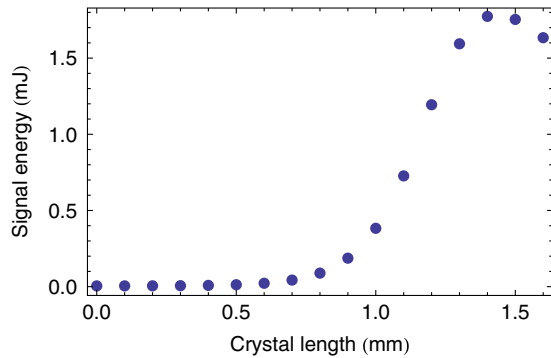


FIG. 8. Calculated amplified $2\ \mu\text{m}$ pulse energy as a function of crystal length of the second optical parametric amplifier. The input pump energies of the signal and pump are $1\ \mu\text{m}$ and $10\ \text{mJ}$, respectively, pulses have transform-limited $50\ \text{fs}$ FWHM duration, and the beams are fourth-order super-Gaussian with $1/e^2$ full width of $10\ \text{mm}$.

typically result in efficiencies on the order of 20% (Fig. 8). Thus, we can expect that with $10\ \text{mJ}$ pump pulses we can produce $1.5\text{--}2\ \text{mJ}$ pulses at $2\ \mu\text{m}$. The predicted optimal crystal length for the second optical parametric amplifier is $1.4\ \text{mm}$. While the presented optical system contains many elements, the overall attenuation would result in a negligible reduction of the pulse energy from the system. The reason for this is the fact that the OPCPA system operates in the region of pump pulse depletion, where the output energy of the second OPA is relatively insensitive to its seed pulse energy, i.e., the optical losses in the system.

In Fig. 9 we show the effect of signal and pump beam reshaping in the final optical parametric amplifier, respectively, with the chosen crystal length of $1.4\ \text{mm}$. While the signal maintains a super-Gaussian shape, the spot size is somewhat reduced due to the considerably lower parametric gain near the beam edge. Significant pump depletion is predicted with the chosen beam size, which indicates a good conversion efficiency can be achieved.

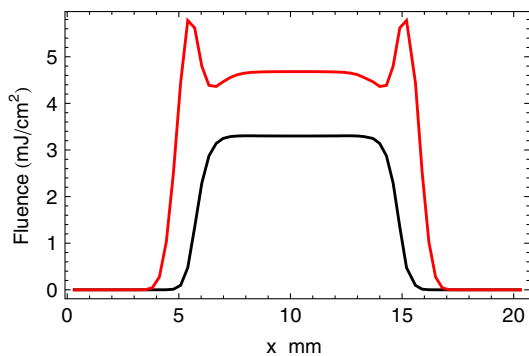


FIG. 9. Signal (black) and pump (red) beam profile after the second optical parametric amplifier, for a crystal length of $1.4\ \text{mm}$.

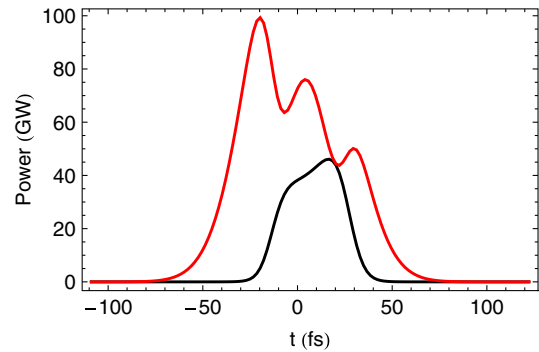


FIG. 10. An improved temporal profile calculation for the signal (black) and residual pump (red) after the $1.4\ \text{mm}$ long second optical parametric amplifier by inclusion of group velocity dispersion reveals the temporal walk-off between the pulses and a small shortening and distortion of the amplified signal pulse.

A refined temporal model obtained by including the effects of group velocity dispersion results in a better estimate of the resulting pulse shape and duration following the second optical parametric amplifier. With an assumption of a $50\ \text{fs}$ Gaussian input signal pulse from the first optical parametric amplifier, a modest pulse shortening and distortion is expected, as shown in Fig. 10. The pump depletion is also evident in the pump temporal profile.

IV. EXPERIMENTAL METHODOLOGY

A standard, compact $800\ \text{nm}$ Ti:sapphire laser system will be used to produce pulses with energies of up to $25\ \text{mJ}$, with pulse durations of $\sim 20\ \text{fs}$. These systems are now commercially available and sufficiently robust for long-term facility operation at high repetition rate (up to $1\ \text{kHz}$). A small portion of the pulse ($< 1\ \mu\text{J}$) will be split from the main laser pulse and injected into a SPM stage, while the remainder will be used to pump two OPCPA stages.

A low repetition rate Ti:sapphire laser system will be used as a pump for initial proof-of-principle experiment at Penn State University (Amplitude Technologies Trident X based system, $16\ \text{mJ}$, $35\ \text{fs}$, $10\ \text{Hz}$) with the main goal to develop a robust OPCPA prototype capable of delivering $2\ \mu\text{m}$ seed that meets the ESASE requirements. Once the OPCPA technique is tested and optimized, a more powerful Ti:sapphire laser system with repetition rate matched to that of the SLAC LCLS (up to $120\ \text{Hz}$) will be acquired, mated to the OPCPA prototype and installed at SLAC.

From the dispersion standpoint, the two unique aspects of our approach are the generation of the idler beam at $2\ \mu\text{m}$ in the first stage of OPCPA and the use of chirped-pulse pumping. The combination of those two techniques will result in production of a $2\ \mu\text{m}$ pulse with small

negative instead of the positive dispersion. This is similar to some of the recent approaches taken in the OPCPA community and has the additional unique advantage of allowing pulse compression using the normal dispersion of transparent dielectrics. For example, the use of a block of glass of optimally designed thickness will provide the compensatory positive dispersion needed to compress the pulse close to the transform limit. Since the use of material dispersion will not provide ideal dispersion compensation up to the high dispersion orders, it is anticipated that the use of chirped mirrors will also be pursued. Only a small compensation via chirped mirrors, or solid blocks of glass, is anticipated. In effect, this is an OPCPA process with a very small degree of pulse stretch. Some pulse stretching is also needed for the pump, which will be realized using a block of dispersive material (glass), or incomplete pulse compression from the pump laser.

The dispersion compensation scheme will be carefully analyzed and tested experimentally during the initial proof-of-principle experiment at Penn State University. The measurement will be performed using a standard spectral interferometry for direct E-field reconstruction (SPIDER) technique, which will allow the exact specification of the dispersion compensator. Given the relatively small overall dispersion in the system (sub-cm total OPA length), dispersion compensation to near transform limit (20–50 fs) is anticipated to be relatively simple in this regime of pulse durations. We note however that, in order to successfully implement an even shorter short pulse regime of operation (approaching a few optical cycles), we need to carefully analyze not only the amplitude but also the phase characteristics of amplification in OPCPA in more detail to ensure proper dispersion compensation.

V. SUMMARY

A novel ultrafast OPCPA-based laser system operating at 2 μm has a great potential to be beneficial to future ESASE efforts at facilities such as SLAC LCLS. A novel experimental design has been described which has notable advantages compared to prior approaches to production of energetic 2 μm pulses. Most notably, the approach utilizes only commercial Ti:sapphire pump laser technology, and is anticipated to result in compact, robust, and reliable laser system for ESASE.

ACKNOWLEDGMENTS

We wish to express our gratitude to A. Zholents of Argonne National Laboratory for his support of our efforts. This work was performed under U.S. Department of Energy Grant No. DE-SC0004461.

-
- [1] Linac Coherent Light Source Conceptual Design Report No. SLAC-R-593, 2002.
 - [2] P. Emma *et al.*, *Nat. Photon.* **4**, 641 (2010).
 - [3] E. Schneidmiller and M. Yurkov, TESLA FEL Report No. 2010-06, DESY, 2010.
 - [4] M. Altarelli *et al.*, TESLA FEL Report No. 2006-097 DESY, 2006.
 - [5] SPring-8 Compact SASE Source Conceptual Design Report (2005) [<http://www-xfel.spring8.or.jp>].
 - [6] A. Zholents, *Phys. Rev. ST Accel. Beams* **8**, 040701 (2005).
 - [7] A. Zholents, W. Fawley, P. Emma, Z. Huang, G. Stupakov, and S. Reiche, in *Proceedings of FEL2004 Conference* (Comitato Conferenze Elettra, Trieste, Italy, 2004) p. 582.
 - [8] L. C. Steinhauer and W. D. Kimura, *Phys. Rev. ST Accel. Beams* **2**, 081301 (1999).
 - [9] X. Gu *et al.*, *Opt. Express* **17**, 62 (2009).
 - [10] I. Jovanovic, C. Haefner, B. Wattellier, and C. P. J. Barty, *Opt. Lett.* **31**, 787 (2006).
 - [11] BBO specifications provided by Cleveland Crystals, Inc. (2010) [<http://www.clevelandcrystals.com/BBOLBO.htm>].
 - [12] Y. Tang, I. N. Ross, C. Hernandez-Gomez, G. H. C. New, I. Musgrave, O. V. Chekhlov, P. Matousek, and J. L. Collier, *Opt. Lett.* **33**, 2386 (2008).
 - [13] Q. B. Zhang, E. J. Takahashi, O. D. Mucke, P. X. Lu, and K. Midorikawa, *Opt. Express* **19**, 7190 (2011).
 - [14] I. Jovanovic, Ph.D. thesis, University of California, Berkeley, 2001.
 - [15] I. Jovanovic, B. J. Comaskey, and D. M. Pennington, *J. Appl. Phys.* **90**, 4328 (2001).
 - [16] I. Jovanovic, J. R. Schmidt, and C. A. Ebberts, *Appl. Phys. Lett.* **83**, 4125 (2003).
 - [17] I. Jovanovic, C. A. Ebberts, and C. P. J. Barty, *Opt. Lett.* **27**, 1622 (2002).
 - [18] I. Jovanovic, B. J. Comaskey, C. A. Ebberts, R. A. Bonner, D. M. Pennington, and E. C. Morse, *Appl. Opt.* **41**, 2923 (2002).
 - [19] I. Jovanovic, C. A. Ebberts, B. C. Stuart, M. R. Hermann, and E. C. Morse, in *Conference on Lasers and ElectroOptics, Trends in Optics and Photonics* (Optical Society of America, Washington, DC, 2002), Vol. 73, p. 387.
 - [20] Available from A. V. Smith, SNLO Nonlinear Optics Code, Sandia National Laboratories, Albuquerque, NM.